

Potential Driving Systems Associated with Extreme Rainfall across East Africa during October to December (OND) Season 2019

Constantine Ingeri^{1,2*}, Wang Wen¹, Joseph Ndakize Sebaziga^{3,4,5}, Vedaste Iyakaremye², Samuel Ekwacu^{4,6}, Prosper Ayabagabo², Anthony Twahirwa^{2,7}, Jonah Kazora^{1,2}

¹School of Atmospheric Sciences, Nanjing University of Information Science and Technology, Nanjing, China

²Rwanda Meteorology Agency (Meteo Rwanda), Kigali, Rwanda

³School of Science and Technology, University of Rwanda (UR-CST), Kigali, Rwanda

⁴Climate and Clean Air Coalition Secretariat, Paris, France

⁵Rwanda Environment Management Authority (REMA), Kigali, Rwanda

⁶Uganda National Meteorological Authority (UNMA), Kampala, Uganda

⁷Department of Earth and Climate Science, University of Nairobi, Nairobi, Kenya

Email: *c.ingeri@meteorwanda.gov.rw, *constaingeli@gmail.com

How to cite this paper: Ingeri, C., Wen, W., Sebaziga, J. N., Iyakaremye, V., Ekwacu, S., Ayabagabo, P., Twahirwa, A., & Kazora, J. (2024). Potential Driving Systems Associated with Extreme Rainfall across East Africa during October to December (OND) Season 2019. *Journal of Geoscience and Environment Protection*, 12, 25-49.

<https://doi.org/10.4236/gep.2024.127003>

Received: May 21, 2024

Accepted: July 15, 2024

Published: July 18, 2024

Copyright © 2024 by author(s) and Scientific Research Publishing Inc.

This work is licensed under the Creative Commons Attribution International License (CC BY 4.0).

<http://creativecommons.org/licenses/by/4.0/>



Open Access

Abstract

The East African (EA) region highly experiences intra-seasonal and inter-annual variation in rainfall amounts. This study investigates the driving factors for anomalous rainfall events observed during the season of October-November-December (OND) 2019 over the region. The study utilized daily rainfall data from Climate Hazards Group InfraRed Precipitation with Station Data Version 2 (CHIRPSv2) and the driving systems data. Statistical spatiotemporal analysis, correlation, and composite techniques were performed to investigate the teleconnection between OND 2019 seasonal rainfall and global synoptic climate systems. The findings showed that the OND 2019 experienced seasonal rainfall that was twice or greater than its seasonal climatology and varied with location. Further, the OND 2019 rainfall showed a positive correlation with the Indian Ocean Dipole (IOD) (0.81), Nino 3 (0.51), Nino 3.4 (0.47), Nino 4 (0.40), Pacific Decadal Oscillation (PDO) (0.22), and North Tropical Atlantic (NTA) (0.02), while El Nino-Southern Oscillation (ENSO) showed a negative correlation (-0.30). The region was dominated by southeasterly warming and humid winds that originated from the Indian Ocean, while the geopotential height, vertical velocity, and vorticity anomalies were closely related to the anomalous rainfall characteristics. The study deduced that the IOD was the major synoptic system that influenced maximum rainfall during the peak season of OND 2019. This study therefore provided insights on the diagnosis study of OND 2019 anomalous rainfall and its attribu-

tion over the EA. The findings of the study will contribute to improvements in forecasting seasonal rainfall by regional climate centers and national meteorological centers within the region.

Keywords

East Africa, Driving Climate Systems, October-November-December (OND) 2019 Rainfall

1. Introduction

The 21st century has witnessed an increase in extreme weather events and climate variability, including droughts, torrential rains, and floods. These events lead to water and food shortages, energy deficits, and socio-economic disruptions (Woodward et al., 2016). East Africa (EA) is one of the regions of Africa with high intra-seasonal to inter-annual rainfall variability (Lüdecke et al., 2021). The EA experiences rainfall bimodality, with the short rainy season extending from October-November-December (OND) being noted for its exceptionally extreme rainfall (Doi, Behera, & Yamagata, 2022; Wainwright et al., 2020). During OND 2019, EA witnessed a crucial period where several parts of the region experienced one or more extreme rainfall events due to its variability in occurrence and intensity compared to the previous rainfall (Lüdecke et al., 2021; Woodward et al., 2016). Over the region, rainfall is the climate variable with the most impacts, where above-normal rainfall events result in extreme rainfall events such as flooding and landslides, among others, while the deficit results in dry spells, which may lead to drought and consequently famine (Krüzselyi et al., 2011; Shrivastava & Umar, 2023). EA rainfall variability is linked to various driving systems associated with the patterns of sea surface temperatures (SSTs) over the Indian, Pacific, and tropical Atlantic Oceans and regional wind circulations (Roy, Mliwa, & Troccoli, 2023; Varada, 2005). These global synoptic phenomena include and are not limited to the Indian Ocean Dipole (IOD) (Black, 2005; Finney et al., 2020; Palmer et al., 2023; Wainwright et al., 2020), the El Niño-Southern Oscillation (ENSO) (Indeje, Semazzi, & Ogallo, 2000; Nicholson, 2017; Ogallo, 1988; Palmer et al., 2023; Vashisht & Zaitchik, 2022), Atlantic variability (McHugh & Rogers, 2001), zonal equatorial easterlies (Jury, Matari, & Matitu, 2009), and the Southern Annular Mode (SAM) (Mbigi & Xiao, 2023).

Previous studies pointed out that natural disasters across the EA region are often associated with the concurrence of two driving systems, such as IOD and ENSO (Indeje et al., 2000). These two driving systems are linked with increased rainfall over EA (Behera, 2019; Onyutha, 2016), resulting in inter-annual and seasonal variability as well as the occurrence of extreme rainfall events (Indeje et al., 2000; Shilenje & Ogwang, 2015). The excessive reduction of rainfall across EA was identified to be related to the positive and negative IOD events that are

associated with above- or below-average rainfall (Doi et al., 2022; Kebacho, 2021). Additionally, climate change may contribute to more frequent, strong positive IOD events and wet OND seasons (Nicholson, 2019). A reversal in the atmospheric circulation and SST coupled with climatic factors of the atmospheric and ocean phenomenon known as the ENSO over the Tropical Eastern Pacific Ocean is highly linked to the inter-annual variability of the OND season (Dieppois, Rouault, & New, 2015). The rainfall fluctuations showed strong linkage with the ENSO phenomenon, where rainfall tends to be above average during El Niño years with a stronger connection to large-scale atmospheric and oceanic variables than to the local circulation (Nicholson, 2019). Three Niño indices, namely Niño 3.4, Niño 3, and Niño 4, are often used to describe ENSO indices and have a significant impact on the variability of rainfall over EA (Ren, Zuo, & Deng, 2019). Further, the Inter-Tropical Convergence Zone (ITCZ), referred to as a short band of strong precipitation that surrounds the Earth at the equator (Green, Marshall, & Donohoe, 2017), and its position appear to have an impact on the variability of rainfall over the EA. There is high dependence on the ITCZ latitudinal position and the seasonal meridional SST gradient between the tropical North and South Atlantic. The North Tropical Atlantic also plays a big role in OND seasonal rainfall due to the ITCZ position in the North during the OND season. There is a strong linkage to inter-annual rainfall variability over Southeastern Africa with the North Atlantic Ocean, and the Southeastern African ITCZ shifts southward (northward) when the North Atlantic westerlies are unusually strong (weak) (Eichhorn & Bader, 2017). Other studies suggest that the anomalous wet rainfall in EA occurs during periods of westerly out-breaks bringing moist Atlantic air into the EA region (McHugh & Rogers, 2001; Otieno et al., 2018; Philippon et al., 2016). Additionally, the North Tropical Atlantic is indeed a factor that contributes to East Africa's rainfall variability. The SST anomalies in the tropical Atlantic play a big role in influencing rainfall patterns in EA, particularly through their impact on zonal winds and atmospheric circulation (Liu et al., 2014; Moron, 1997), which highlights the importance of zonal winds over the tropical Atlantic in modulating rainfall in West Africa and their downstream effects on East African precipitation patterns. NTA influences OND rainfall through the warm SST anomalies that occur during August, September, and October. The North Atlantic Ocean is also one factor contributing to the Madden-Julian Oscillation (MJO) modulation of EA rainfall. The MJO, operating at a sub-seasonal time scale, interacts with the ENSO and can lead to increased potential for daily precipitation excesses during wet MJO phases under El Niño conditions (Balaguru et al., 2021). The multi-decadal Pacific Decadal Oscillation (PDO) is a fluctuation in the tropical and mid-latitude North Pacific SST that is characterized by cooler central North Pacific SSTs and warmer west coast SSTs during its positive and negative phases (McHugh & Rogers, 2001; Yang et al., 2022). Tropical Pacific SST directly affects African rainfall through shifting the Walker Circulation in the Indian Ocean (Alexander et al., 2002; Black, Slingo, & Sperber, 2003), and indirectly through the tropical Atlantic

SST's characteristic (Latif & Grötzner, 2000; Nicholson & Selato, 2000). The PDO coincides with rainfall for several countries in the EA, particularly from October through December (Preethi et al., 2015). These driving systems, coupled with SST variations, have a significant impact on the rainfall patterns over EA, and they are among the leading natural climate indices that have a strong impact on global and regional average temperature and rainfall (Pohlmann & Latif, 2005; Zhang & Delworth, 2006). Other teleconnections that influence the rainfall over EA are tropical storms, easterly waves, jet streams, and extra-tropical weather systems (Ogallo, 1989).

Extreme rainfall events, such as the OND, 2019 in EA, have caused severe economic and societal impacts. Efforts have been made to unravel the semantics behind OND 2019 rainfall dynamics (Kai, Kijazi, & Osima, 2020; Kebacho, 2022; Nicholson et al., 2022; Wainwright et al., 2020). However, this study provides a comprehensive diagnostic analysis of global synoptic climate systems (IOD, ENSO, Nino indices, PDO, and NTA), aiming at discerning the individual contributions and effects of these systems on the extreme rainfall experienced during the OND 2019 season in the EA region. After the introduction, the piece of work studied here is subdivided into three sections, where section one presents the data and methodology, section two discusses the result, and the conclusion and recommendations are presented in section three.

2. Study Area, Data and Methodology

2.1. Study Area

East Africa (EA) is located in the equatorial belt with a geographical coordinate of 11.72°S-5.1°N latitude and 28.7°E-41.91°E longitude as it is shown in **Figure 1**. It has five countries: Rwanda, Burundi, Uganda, Tanzania, and Kenya. The topography of EA is remarkable; there is the East African Rift Valley created by global plate tectonic forces; numerous mountains with high elevation in Africa like Mount Kilimanjaro (5895 m) and Mount Kenya (5197 m); various water bodies cover up some parts of the region like Lake Victoria, Lake Tanganyika, Lake Albert, Lake Turkana, and Lake Kivu.

Due to the region's tropical climate, which is distinguished by severe seasonality in rainfall and wet and dry seasons as opposed to the four-season pattern observed in other regions of the world, EA has both wet and dry seasons. Refer to **Figure 2** below.

2.2. Data

The daily gridded rainfall data for a period of 30 years (1991-2020) were sourced from the Climate Hazards Group InfraRed Precipitation with Station Data Version 2 (CHIRPSv2). The CHIRPS dataset is widely used due to its exceptional performance over the greater Horn of Africa (Chang'a et al., 2020; Ngoma et al., 2021). It incorporates 0.05° × 0.05° resolution satellite imagery with in situ station data to create gridded rainfall time series suitable for intra-seasonal variability

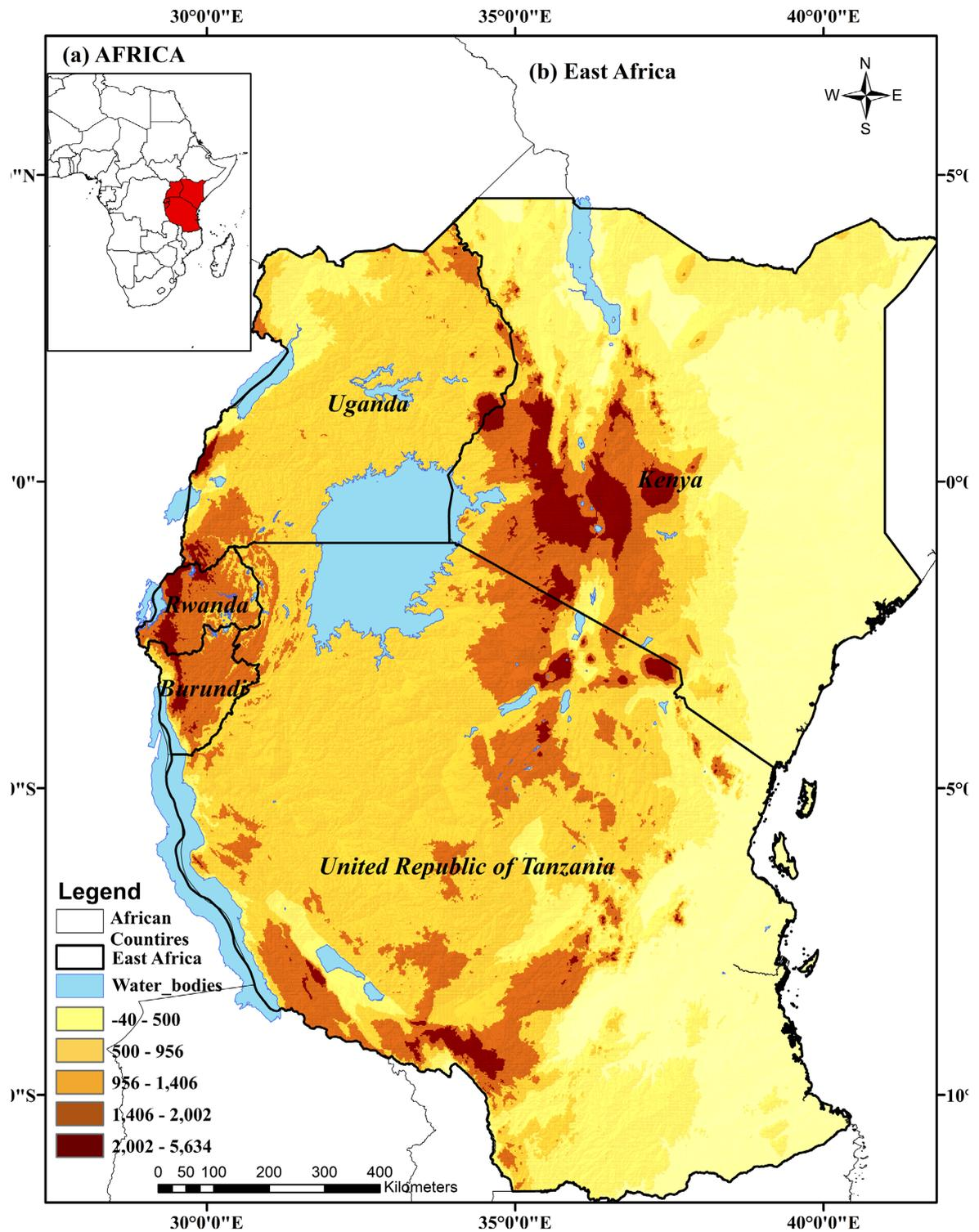


Figure 1. The geographical location of East Africa.

analysis, and they are highly blended with the gauge or observed data in situ (Kavishe & Limbu, 2020). The driving systems time series dataset of DMI The Hadley Centre Global Sea Ice and Sea Surface Temperature (HadISST1.1), which is the dipole mode index representing the Indian Ocean Dipole (IOD), is defined

as the SST anomaly difference between the western (10°S-10°N, 50°-70°E) and eastern (10°S-0°, 90°-110°E) tropical Indian Ocean. To compute the South Oscillation Index (SOI), representing the El Niño-Southern oscillation (ENSO), the SST anomalies in the eastern equatorial Pacific are obtained from the Climate Research Unit (CRU) website. We used Niño 3.4 located at (5N-5S, 170W-120W), Niño 3 located at (5°S-5°N, 150°W-90°W), Niño 4 located at (5N-5S, 160E-150W), Pacific Decadal Oscillation (PDO) and North Tropical Atlantic (NTA) obtained from SSTs in Atlantic Ocean at the coordinates 60W-20W, 6N-18N and 20W-10W, 6N-10N, Data is obtained from the Extended Reconstruction SST Version 3 (ERSSTV3b) dataset. SSTs and relative humidity used are obtained from the National Oceanic and Atmosphere Administration (NOAA). The geopotential height, vertical velocity, and vorticity datasets are from ECMWF Reanalysis v5 (ERA5).

2.3. Methodology

The daily rainfall dataset was subjected to both temporal and spatial analysis in order to identify rainfall variability over the EA. In order to verify the OND season rainfall and the excessive rainfall of the OND 2019 season, we investigated the rainfall amounts of OND 2019 for various regions compared to the long-term mean. Pearson's correlation analysis was used to determine the specific impact of each driving system on the rainfall variability in EA. The association between the OND season rainfall during wet years over EA and the IOD, ENSO, Niño 3.4, Niño 3, Niño 4, PDO, and NAO indices was determined. The years with high positive rainfall anomalies during the OND period were expressed as wet years, as shown by the temporal time series. Pearson's correlation is performed by calculating Pearson's correlation coefficient r , known as the correlation coefficient, which is defined as a measurement quantifying the strength of the association between Rainfall and driving systems, with values ranging from -1 to +1 indicating a strength of linear relationship between them, whereas a value of 0 indicates no linear relationship.

$$r = \frac{n(\sum xy) - \sum x \sum y}{\sqrt{[n(\sum x^2) - (\sum x)^2][n(\sum y^2) - (\sum y)^2]}}$$

where, x represents driving systems, y represents the OND rainfall, n is the sample size, and \sum represents a summation for n -values. Pearson's correlation coefficient r calculated shows the relationship between OND rainfall 2019 over East Africa with these driving systems; Indian Ocean Dipole (DMI), The El-Niño South Oscillation (ENSO), Niño 3.4, Niño 3, Niño 4, Pacific Decadal Oscillation (PDO) and Atlantic Oscillation (NAO) index. The P-values, with 0.05 significance level, were calculated to accept (reject) the statistical significance of the correlation between OND rainfall and driving systems. The null hypothesis was that the value of r in n -values was zero. If the calculated P-value was less than 0.05, the null hypothesis H_0 (no correlation) would be rejected and vice versa; if

P-value > 0.05, it means the correlation would be statistically significant. This method was widely used by different researchers (Dezfuli & Nicholson, 2013; King'uza & Limbu, 2019; Nicholson & Dezfuli, 2013), and (Muthoni et al., 2019) when they correlated the tropical sea surface temperature (SST) and rainfall.

The composite analysis conducted in this research looked at how large-scale global teleconnections affect atmospheric variability. This approach has been widely used by researchers to gain deep insights into weather patterns and extreme climate events, as well as to better understand and diagnose the state of the climate system on a regional and global scale (Dezfuli & Nicholson, 2011; Gunta & Bhat, 2022; Ogwang et al., 2015). In order to illustrate the atmospheric circulation over the area, the remapped sea surface temperature and rainfall composite for OND 2019 associated with wind were analyzed to understand the wind patterns during this period, and at the same time, the relative humidity, geopotential height, and vorticity composite were analyzed for further insight into the atmosphere at various levels. associated with wind was analyzed to illustrate the wind patterns during this period, and at the same time, the relative humidity, geopotential height, and vorticity composite were analyzed for further insight into the atmosphere at various levels.

3. Result

Figure 2 presents the rainfall for October-November-December (OND) long-term mean, OND 2019 and OND rainfall averaged over the EA. The long-term mean rainfall distribution (**Figure 2(a)**) shows that the western side of the region receives a relatively high amount of rainfall (400 - 600 mm). The central parts of Tanzania and the northern parts of Kenya experience a low amount of rainfall (0 - 200 mm), while the rest of the region shows a moderate amount of rainfall (200 - 400 mm). Compared to the long-term mean, the OND 2019 (**Figure 2(b)**) witnessed above-normal rainfall over most parts of the EA region. The observed rainfall during OND 2019 was not evenly distributed; some regions experienced a high amount of rainfall while others experienced extremely above-normal rainfall over the EA region. The areas that experienced heavy rainfall during OND 2019 can be split into three parts: region A, which lies around Lake Victoria and is south-eastern Uganda and northwestern Tanzania; region B, which is located in the central and southern parts of Kenya; and region C, which is located in the northern coast of Eastern Tanzania that borders the Indian Ocean. These representative areas were chosen in contrast to other EA regions, which are known for having heavy rainfall. The map shown in **Figure 2(a)** indicates the long-term mean of OND rainfall. Typically, region A, located around Lake Victoria, and region B, located in central South Kenya, recorded the highest rainfall compared with other regions. **Figure 2(b)** illustrates the OND 2019 rainfall. The whole region was experiencing above-normal rainfall, especially regions A, B, and C, which would have more complex spatial rainfall modes during the short rainfall season of OND 2019, due to the influence of the complex regional physical features contributing to the above-normal

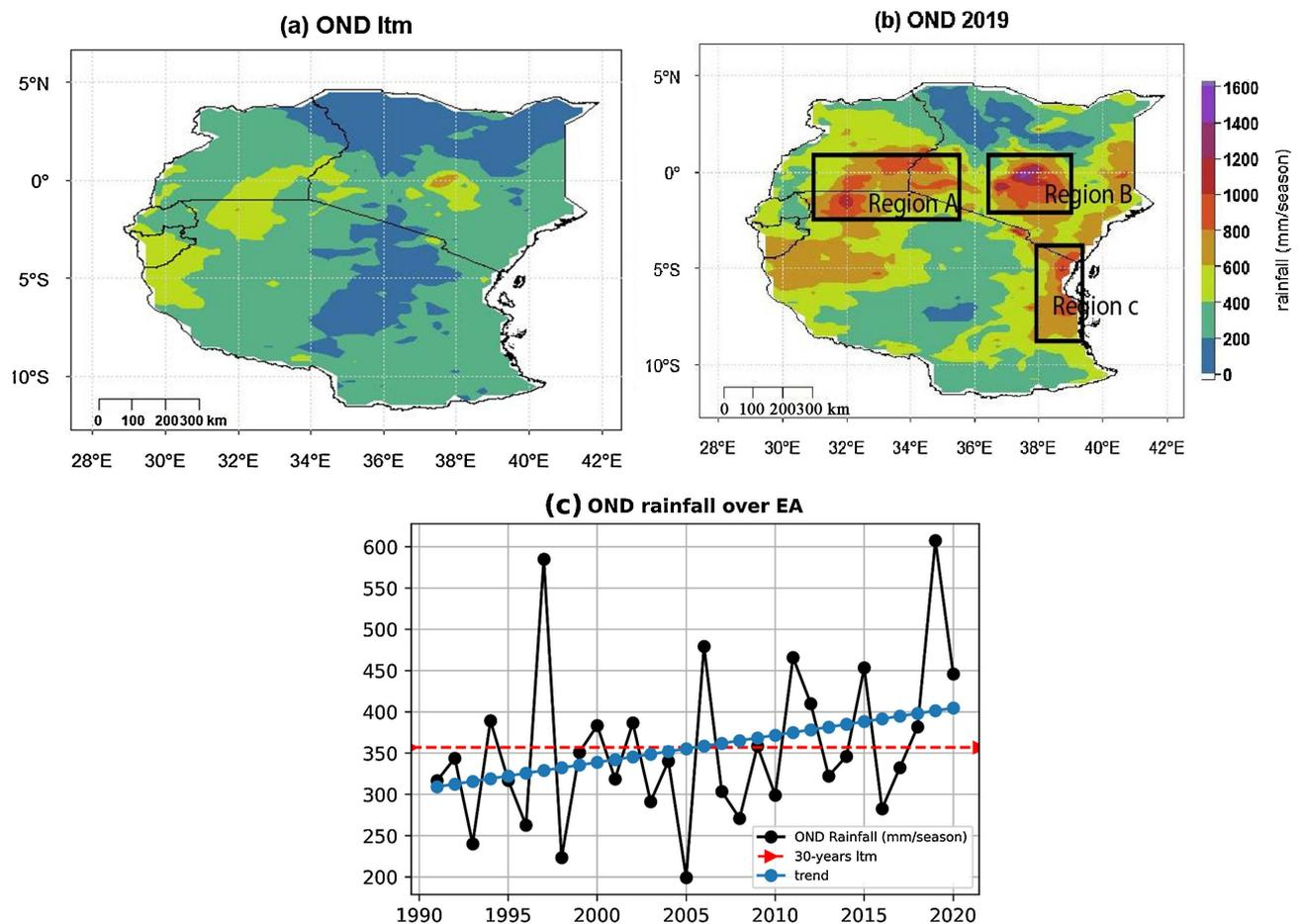


Figure 2. The spatial distribution of (OND) of season rainfall for: (a) the long-term mean (ltm) seasonal rainfall, (b) the OND 2019 seasonal rainfall and (c) trend of seasonal averaged rainfall over East Africa during October-November-December from 1991 to 2020.

rainfall, which is associated with increased local circulation in the regions. For instance, the area-averaged rainfall of central Kenya (region B) has the highest rainfall, approximately 130% (900 mm) above the climatological average for the OND season. **Figure 2(c)** illustrates the time series of OND rainfall. Over EA over 30 years since 1991 to 2020, generally the whole region of East Africa indicates an increase in rainfall for the OND period. As there has been a decline in rainfall for some years, the OND 2019 had 600 mm/season averaged rainfall over the whole region of EA, as the mean is estimated to be around 355 mm/season.

Considering different locations over the EA, the inter-annual variability of rainfall during the OND season shows a nonhomogeneous characteristic. Some locations, such as the as the central region near Lake Victoria (region A), have anomalies that peak at extremes (530 mm), and the center of Kenya saw abnormally high rainfall with seasonal abnormalities of 590 mm. At the same time, other areas located in the eastern parts of Rwanda received typical rainfall with anomalies of 30 mm for OND 2019.

Figure 3 illustrates the trend of annual OND seasonal rainfall, wet (dry) days, and wet (dry) spells. The analysis of the wetness (days with more than 0.85 mm)

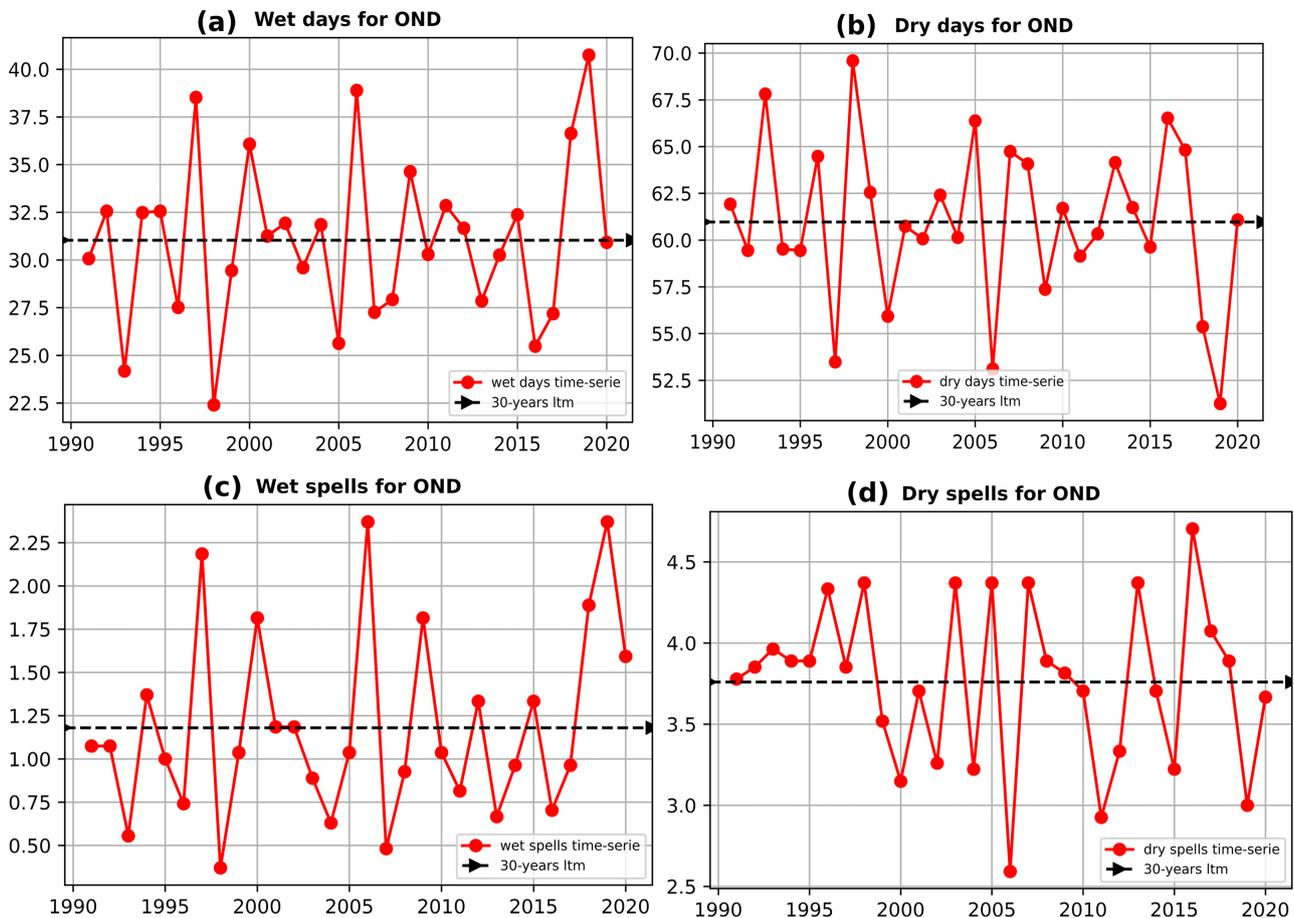


Figure 3. Trend of the wet days (a), dry days (b), wet spell (c), and dry spell (d) during October, November, and December (OND) for 1991-2020 over East Africa.

and dryness (days with less than 0.85 mm) indicates an increasing trend for wet days and wet spells, as well as a decreasing trend for dry days and dry spells. In contrast to previous OND seasons spanning several years, this period has fewer dry days. The wet days for OND 2019 are peaking at more than 40 days, while the dry days are less than 50 days. The wet spell of 5 continuous wet days with a probability of exceeding 400 mm indicates an increasing trend and high value during the period of OND 2019 seasonal rainfall. These results of daily analysis assert the wetness of the OND 2019 season. The resulting OND seasonal rainfall in regions with high daily and monthly rains may cause flooding and landslides like what happened during OND 2019 (Nicholson et al., 2022).

Figure 4 presents the correlation between the OND seasonal rainfall and different driving systems. The driving system includes the Indian Ocean Dipole (IOD), El Niño-Southern Oscillation (ENSO), Nino 3.4, Nino 3, Nino 4, PDO, and NTA. The spatial coherence of OND rainfall with these driving systems is considerable. For instance, the Indian Ocean Dipole (IOD) has a significant influence on the OND seasonal rainfall in EA, with a correlation coefficient ranging from 0.50 to 0.75 (**Figure 4(a)**). The regions A and B show a positive correlation coefficient, particularly the central region encompassing Lake Victoria

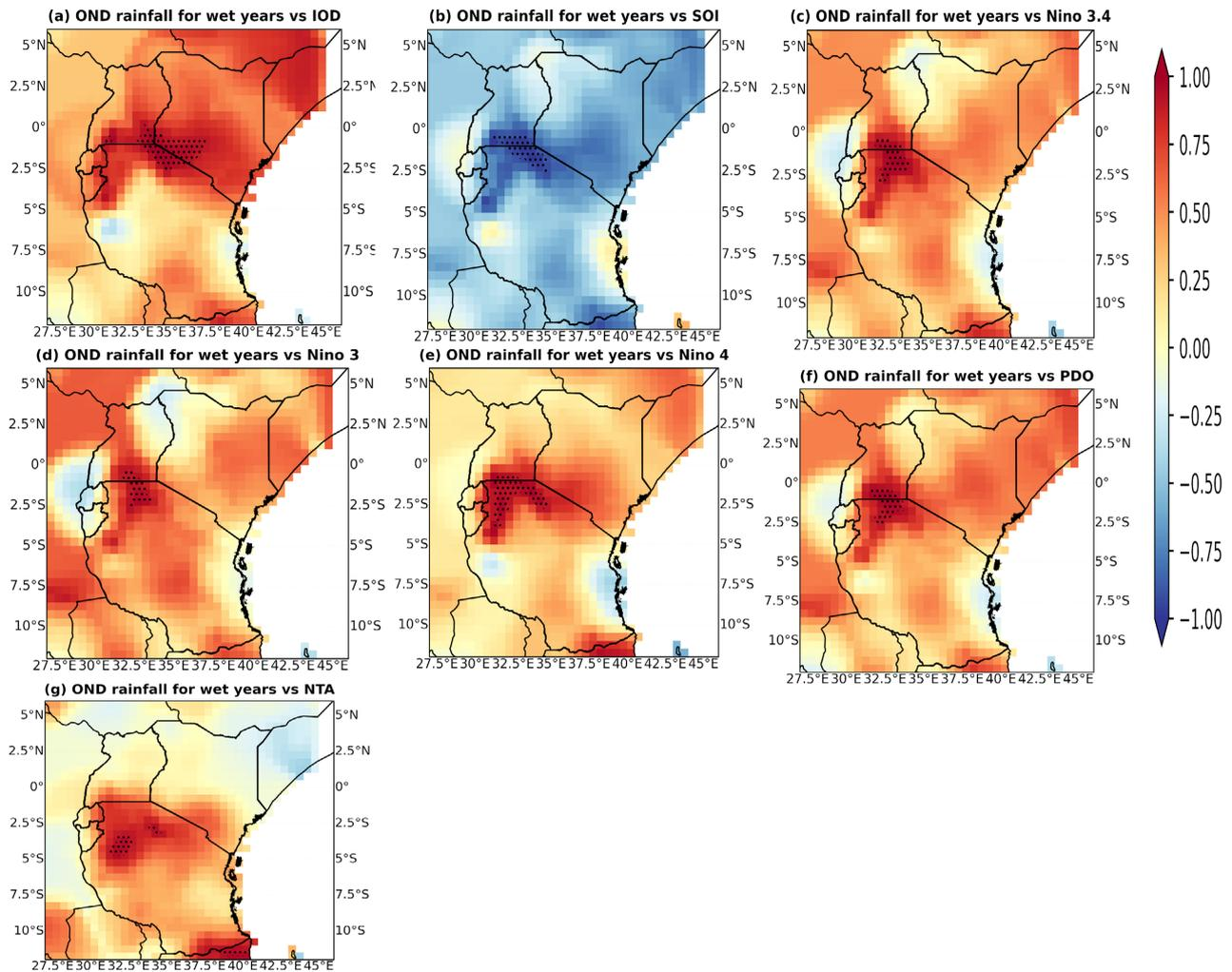


Figure 4. The correlation between the OND seasonal rainfall vs different driving systems.

and Serengeti National Park, which shows a significant positive correlation. The positive IOD results in substantial seasonal rainfall variability due to the El-Nino phase of the IOD, while the negative IOD results in fair association with OND rainfall (supplementary 2). High-altitude regions with numerous water bodies increased the probability of extreme rainfall, such as those in Kenya during OND 2019. The region C, located in the east of Tanzania, exhibited a negative correlation coefficient that fell below 0.25 during wet years, indicating a little impact of IOD on the region's rainfall amounts. The positive correlation coefficient is shown across the rest of the EA region.

The El Niño-Southern Oscillation (ENSO) was associated with OND seasonal rainfall in East Africa (**Figure 4(b)**). The correlation analysis showed a strong negative correlation coefficient over the entire region of East Africa for wet years, with a significant negative correlation coefficient ranged between 0.50 and 0.75 in the central region of EA (region A) and the central south of Kenya (region B), while region C has the positive correlation. There is a negative correlation for the rest of the region. It is known that the influence of ENSO on OND

seasonal rainfall over East Africa is significant (Roy et al., 2023). Typical ENSO-strong El Niño (right) events occur in early spring; the influence of ENSO on OND seasonal rainfall during winter is low, but El Niño events associated with warmer SST anomalies over the central and eastern Pacific result in wet conditions of seasonal rainfall over the region (Müller & Roeckner, 2008). The result validates the relationship between ENSO and OND rainfall, and it also shows that extreme weather occurs across East Africa when positive IOD and the El-Niño phase of ENSO coincide. When it comes to OND seasonal rainfall, DMI and ENSO exhibit great coherence. The DMI has a strong positive correlation, while the ENSO has a strong negative correlation associated with the warming of SSTs over the Pacific Ocean. The OND season rainfall in 2019 is significantly impacted by the ENSO influence.

The OND rainfall in 2019 in East Africa is influenced by other various driving systems, including Nino 3, 4, Nino 3, Nino 4, Pacific Decadal Oscillation (PDO), and North Tropical Atlantic (NTA). The correlation coefficient of these systems is positive, with a significant positive correlation coefficient for regions A and B (Figures 4(c)-(e)). The Nino 3.4 and Nino 3 have equivalent effects; they exhibit similar spatial patterns but differ in terms of intensity; Nino 3.4 shows a high correlation coefficient while Nino 3 and Nino 4 show a low correlation coefficient; overall, the effects of Nino 3.4 over east Africa seem to be more extensive than those of Nino 3. The correlation for region A indicates a very strong positive and substantial correlation coefficient around 0.70 during both Nino 3.4, Nino 3, and Nino 4, for rainy years. The rest of region has a fair positive correlation coefficient for wet years. This suggests that for both wet years, there is a strong and stable association between seasonal rainfall and Nino 3.4 compared to other Nino 3 and 4, but all these Nino indicate a significant positive correlation, which is the fact that they can affect OND rainfall.

The influence of PDO and NTA on the OND rainfall is determined (Figure 4(g), Figure 4(e)). The correlation performed between PDO and OND rainfall confirms the influence of PDO on EA rainfall. The coefficient of correlation of seasonal rainfall with PDO is generally positive for the whole region of EA; region A has a significant positive correlation coefficient ranging around 0.8, while other regions indicate a positive correction coefficient ranging from 0.25 to 0.50. The variability of rainfall with PDO over East Africa is fair. PDO has a significant influence on OND rainfall. There is a correlation between the OND rainfall and NTA; the correlation coefficient is negative, significant, and positive for region A, ranging from 0.50 to 0.60, as is the positive correlation for regions B and C below 0.50. The rest of regions are negative over the north parts of EA, as they are positive for the south part of EA. The association of OND seasonal rainfall with NTA is significant, potentially influencing rainfall for both wet years in EA.

Figure 5 describes the influence of driving systems to OND 2019 rainfall; the driving system indicated the strong relationship with OND rainfall is IOD, the

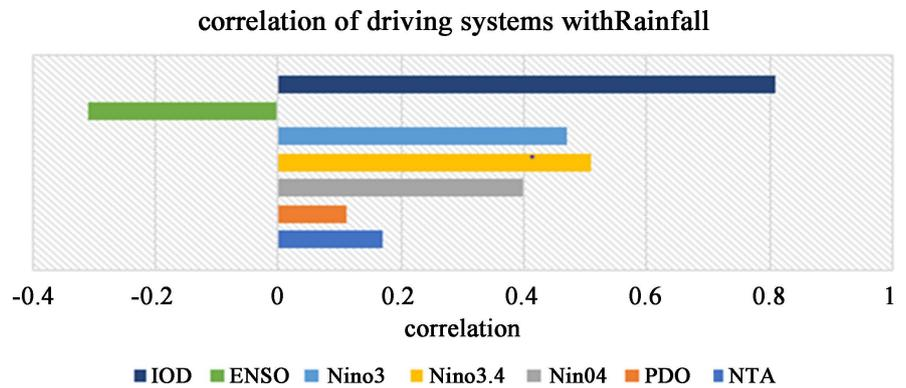


Figure 5. The correlation of OND seasonal rainfall and driving systems.

high and significant positive value of correlation coefficient for IOD is indicated (0.81) as other driving systems have fair values correlation coefficient (Nino 3.4, Nino 3, Nino 4), PDO and NTA have low positive correlation coefficient and ENSO have negative correlation coefficient (**Figure 6**).

Figure 6 illustrates the influence of tropical ocean sea surface temperatures on OND rainfall over the EA region. The driving systems that influence the rainfall over EA are highly sensitive to the SST variability in the Indian Ocean, Atlantic Ocean, and Pacific Ocean. The Indian Ocean is the main source of warm, moist air that influences the atmosphere over the EA (Cai, Chen, & Du, 2022). The association between EA rainfall and Indian Ocean SSTs is well documented (Klein & Goosse, 2018). (Mutai, Ward, & Colman, 1998) investigated the connection between positive IOD occurrences and climate change and concluded that strongly positive IOD events may occur twice as frequently under a world average warming of 1.5°C. Additionally, the western Indian Ocean has recently warmed at one of the fastest rates of any tropical ocean during the past century (Wenegrat et al., 2022). During the OND 2019 season, the eastern parts of the Indian Ocean were cooler at a range of -0.5°C to -1°C to the normal temperature during OND 2019, while the western side of the Indian Ocean was warmed at a range of 1.5°C to 2.0°C (**Figure 6(a)**). This difference in temperature anomaly suggests an increase in positive IOD, which happens to be presumably generating the enhanced rainfall over EA. For the Pacific Ocean, the middle equatorial Pacific SST is warmer than average and colder than average in the areas that generate the driving systems. Warmer SSTs in the western equatorial Pacific and cooler SSTs over the east region of the Pacific Ocean are linked to drier, shorter rains. ENSO weakened and led to a low association with OND rainfall over EA. This content claims that ENSO and OND rainfall have a negative association. The El-Nino phase of ENSO ran at low frequencies during this period, as in the El-Nino years 1997-1998, positive SST anomalies were mainly observed in the eastern tropical Pacific (Vashisht & Zaitchik, 2022). In contrast, there are anomalously increasing SSTs in the central region of the tropical Pacific Ocean. This asserts the positive correlation obtained between different indices of Nino (Nino 3, Nino 3.4, Nino 4) and OND rainfall in 2019. In addition,

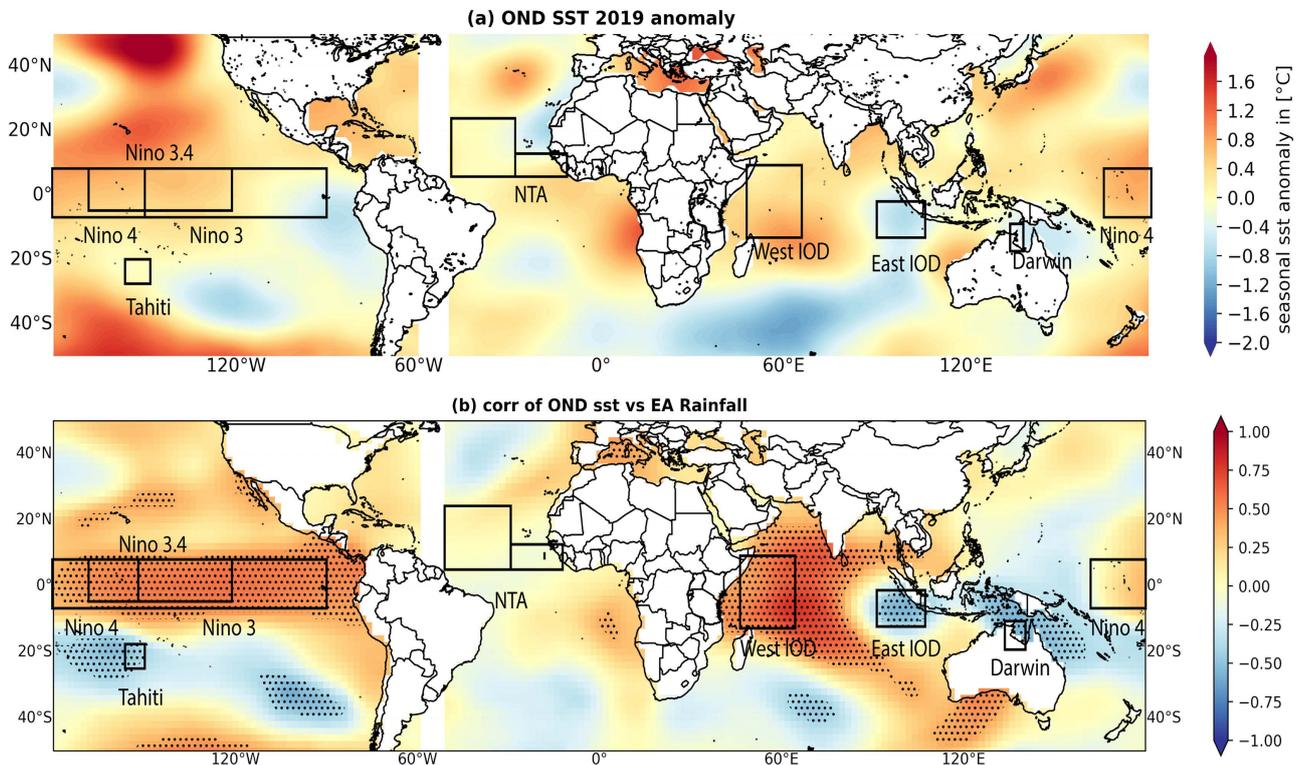


Figure 6. The composite of SST during the OND period (a) OND sea surface temperature temporal trend (b) the sea surface temperature anomaly for OND 2019, the west part of Indian Ocean shows an increase in sea surface temperature anomaly as the east part of Indian Ocean shows a decline in sea surface temperature anomaly.

the propagating feature of the SST anomalies is weaker and less clear in the ENSO region, while it is stronger and very clear in the region of the Nino indices. In the Atlantic Ocean, the location of NTA shows an increase in SSTs and asserts the positive correlation obtained (Figure 3(g)).

To get more insight into the impacts of the impacts of driving systems on OND rainfall, the correlation between SSTs and OND rainfall was carried out and illustrated in Figure 6(b). The results of the correlation analysis reveal a relationship between OND rainfall and SSTs in the driving systems' area. There is a significant and strong positive correlation over the Indian Ocean, particularly in the western region where the positive IOD occurred. Similar to the Pacific Ocean, there is a significant positive correlation over the region of Nino indices, confirming the relationship between Nino indices and OND rainfall in EA. However, the ENSO area and the north tropical Atlantic Ocean exhibit negative correlations, confirming the weak relationship between these driving systems and OND rainfall.

Figure 7 shows the composite analysis of sea surface temperature and OND rainfall related to the zonal wind direction at the surface, with a discernible difference between the composite of the OND long-term mean and that of OND 2019. There is an anomalous equatorial Westerly wind moving the moisture from West to East of Indian ocean and the temperature for the West region is low, as for OND 2019, Anti-Cyclone located in west Indian ocean near East

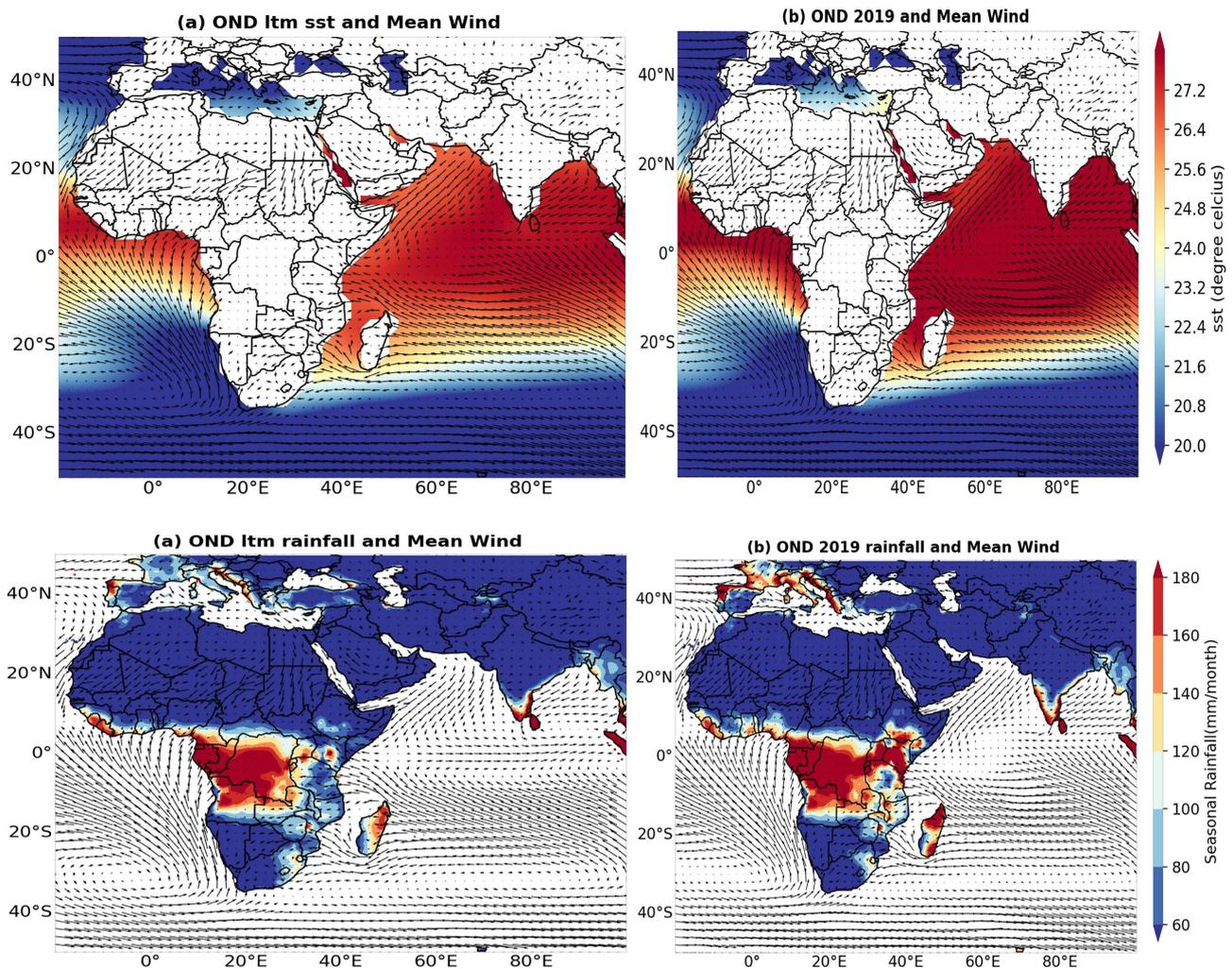


Figure 7. OND Seasonal Sea Surface Temperature and Rainfall vs. Mean Wind Vector Long-Term Mean (Climate) (b) OND Seasonal 2019.

Africa increases sea surface temperature in West tropical region of Indian ocean as it is decreasing to east part, result in increasing the positive IOD and the above-normal rainfall occurred for East Africa region, this anti-cyclone formed in West part of Indian ocean result in strong horizontal gradients of temperature which are particularly favorable for the formation and development of convective atmosphere, this anti-cyclone influence the atmospheric circulation over coastal areas of East Africa as the easterly trade winds moves the moisture from east to west, the sea surface temperature is increased over tropical of Indian Ocean, it may reach over 30°C as it is not exceed the 28°C climatologically, stipulate the above-normal rainfall over EA. For OND 2019, the strong anomalous southeasterly winds from the Indian Ocean strike the majority of the region, and the northeasterly winds estimated at 5 m/s strike the coast of East Africa. There is a strong and consistent easterly wind, projected to be blowing at 8 m/s, moving from the eastern part of the Indian Ocean into East Africa during the OND period. Additionally, there is an anti-cyclone with a low speed of around 2 m/s

in the center, but it increases toward the south and west regions of the Indian Ocean, resulting in enhanced rainfall. However, according to climatology, the strong and steady westerly wind moving toward the eastern region of the Indian Ocean moves the warm and moist air from the west region of the Indian Ocean and avoids the EA from receiving the enhanced rainfall. The outcome shows that the increased rainfall during OND 2019 was brought on by warm, moist South and North-easterly winds, and the development of tropical anti-cyclones in the western Indian Ocean boosts the convective environment over the region of EA.

Figure 8 shows the relative humidity anomalies during the 2019 OND season throughout the land. The climatology period from 1991 to 2020 is used to calculate the season mean climatic anomaly (just the climatological mean subtracted, not normalized). For the period of OND 2019, the relative humidity anomalies are higher over EA. The east and central regions of EA exhibit a positive anomaly with values ranging from 9% to 12%, which suggests an increase in atmospheric humidity. Almost all of the air in these regions is saturated with deep convective inflow, which tends to move upward as the atmosphere warms and prevails in rainfall activities over the region. The increase in relative humidity across EA signifies a rise in the airborne water vapor pressure relative to the amount of water that could be retained as vapor at that temperature. These findings also point to an increase in rainfall across most of the region, particularly in areas that experienced unusually high rainfall during the 2019 OND period.

Figure 9 shows the geopotential height anomalies for the OND 2019. The majority of EA region observed a negative geopotential heights anomaly with strong winds at 850 hPa (**Figure 9(a)**) resulting in convective atmosphere over EA. At middle troposphere levels of 500 hPa, the low geopotential height is also accompanied by strong winds over the central and northern region (the region located around the Lake Victoria, the whole region of Kenya and Uganda), resulting in the presence of storms or troughs over these regions, while the south region (the entire region of Tanzania) has a relatively high geopotential height,

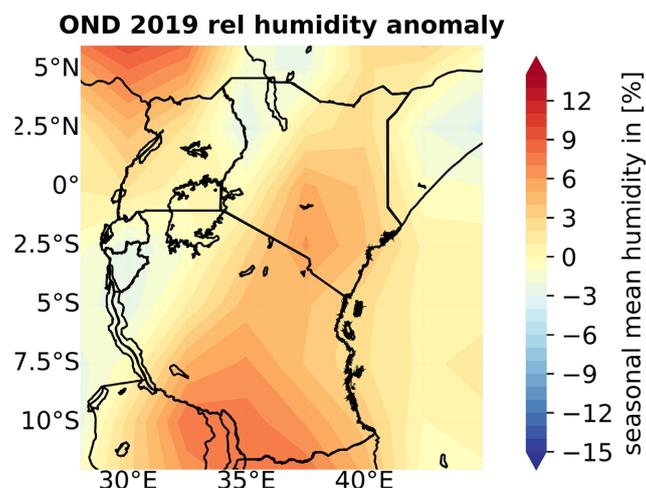


Figure 8. The spatial distribution of season means relative humidity during OND period 2019.

which indicates an inactive and quiescent atmosphere. At the upper level of the troposphere, low geopotential height and strong winds caused storms and unusual rainfall in the central region (the area around Lake Victoria), while high geopotential height and positive geopotential height in the north and south caused ridges and little rainfall in those regions.

Figure 10, illustrated in the vertical velocity composite plotted at various levels of the troposphere, confirms our result; the majority of East Africa's regions depicted negative vertical velocity anomalies. The anomalous low vertical velocity indicates that the clouds and the extreme rainfall are caused by negative anomaly air rising. The majority of East Africa's regions often show that negative vertical velocity anomalies led to unusual rainfall over the area. If moisture is present, areas with large negative values of vertical velocity anomalies will experience heavy rainfall. In the central region, high negative values of vertical velocity are associated with high values of humidity, which led to abnormal rainfall occurring over East Africa. The upward motion of air over the Indian Ocean and the downward motion of air over the nearby continents create numerous vertical

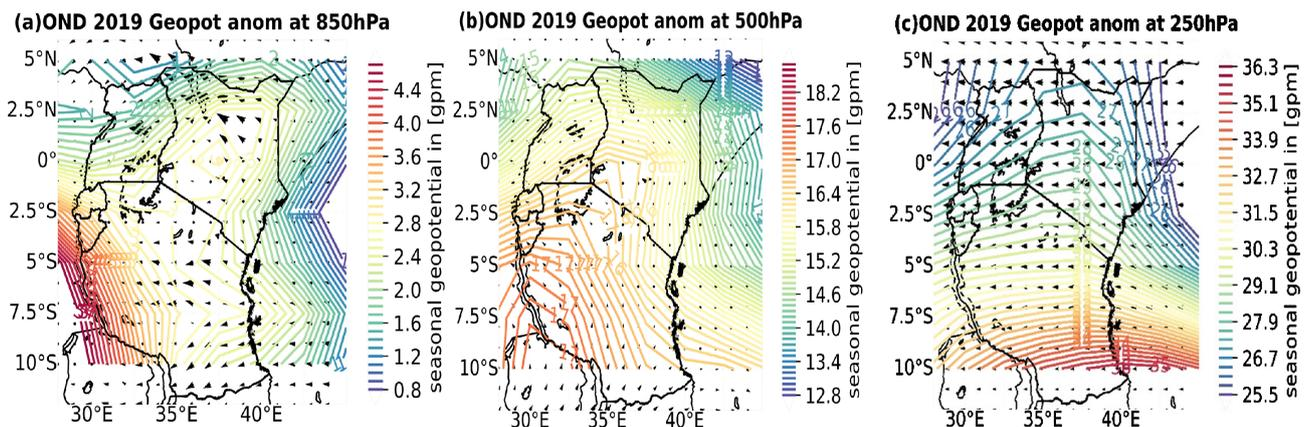


Figure 9. The geopotential height state during the period of OND 2019 seasonal at the different levels (a) 250 hPa (b) 500 hPa (c) 925 hPa.

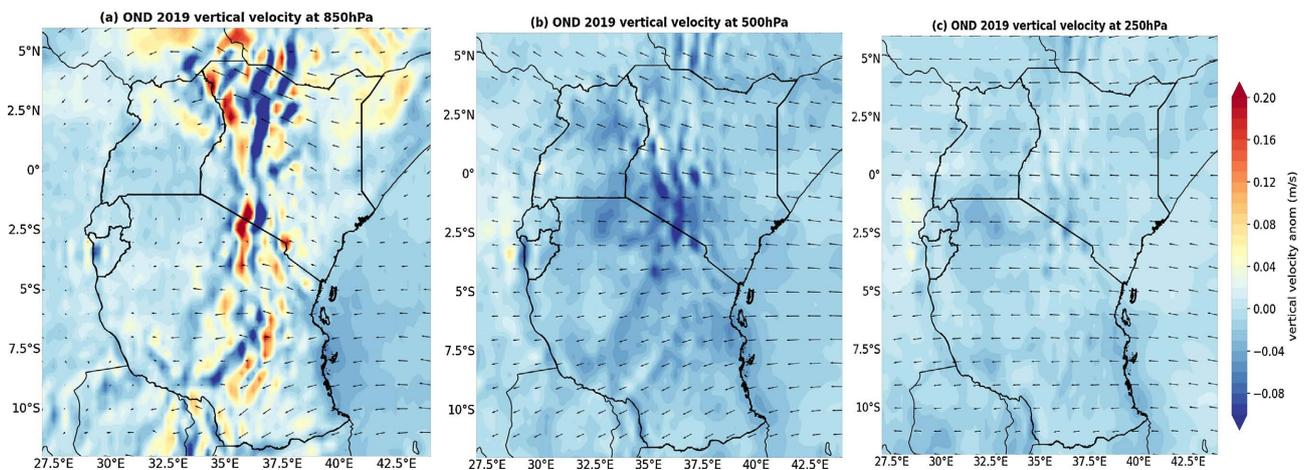


Figure 10. The vertical velocity anomalies with mean wind for the period of OND 2019. (a) at the level of 850 hPa; (b) at the level of 500 hPa; (c) at the level of 250 hPa.

circulations that impact rainfall over the EA and the African continent (KIDSON, 1977; Lyon, 2020)

Figure 11 shows the estimated vorticity anomalies at various levels over the timeframe of OND 2019. In the north hemisphere, the vorticity anomalies are negative and contribute to the enhanced rainfall over the northern part of the EA; the positive vorticity at various levels is linked to storms or anti-cyclones at higher altitudes and tends to correspond with troughs in the geopotential height field. Positive vorticity tends to correspond with ridges in the geopotential height field and is linked to calm weather. The positive vorticity anomaly is located over the south hemisphere over EA, which was increasing from the surface to the upper levels, causing the upper atmosphere to become more dynamically unstable, and the arising wind moves upward in vertical motion, resulting in more activities of rainfall over the south hemisphere. The negative vorticity anomaly over the north hemisphere results in convective atmosphere in the in the East Africa region.

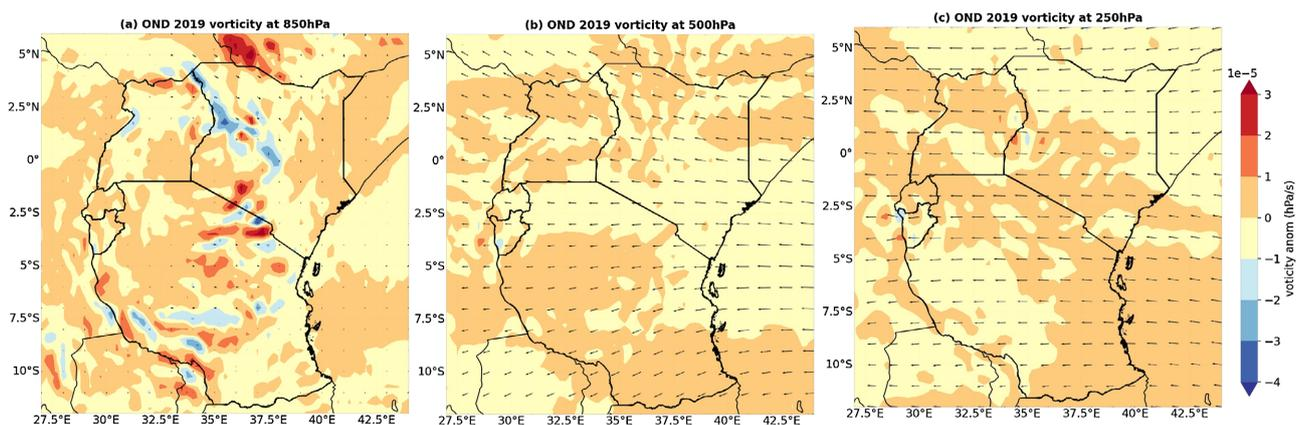


Figure 11. The velocity potential anomaly over the OND seasonal is increasing in East Africa.

4. Discussion

East Africa is one of the parts of Africa with very high rainfall rates due to its location in the tropical zone as mentioned above. The short OND period rainfall shows notable temporal and geographical variation over this century because of global synoptic climate variables that regulate the rainfall across East Africa (Endris et al., 2019; Kolstad & MacLeod, 2022; Ongoma, Chena, & Gaoa, 2018). Numerous studies examined other driving systems, such as IOD, ENSO, and others (Latif et al., 1999; Nyenzi, 1988; Ropelewski & Halpert, 1987), but were not aware of Nino 3.4, Nino 3, Nino 4, PDO, and NTA. All of them were taken into consideration during this investigation in order to conduct additional analysis. For a deeper analysis of the exceptional rainfall of OND 2019, additional features like sea surface temperature, zonal and meridional wind, relative humidity, geopotential height, vertical velocity, and vorticity were examined. The results showed above-normal rainfall during the OND period, with most regions receiving significant amounts of rainfall, as other studies mentioned (Kebacho,

2022; Nicholson et al., 2022; Wainwright et al., 2020), and (Chang'a et al., 2020). However, some regions had normal rainfall below 400 mm/season due to the dispersal of this extreme rainfall. The OND 2019 is twice or three times greater than the climatological rainfall observed over some regions of East Africa.

It was determined how several driving systems, including the Indian Ocean Dipole (IOD), El Nino South Oscillation (ENSO), Nino 3.4, Nino 3, Nino 4, Pacific Decadal Oscillation (PDO), and North Tropical Atlantic (NTA), affected rainfall in East Africa. The findings indicate a strong correlation between East African OND rainfall and driving systems, including IOD, Nino 3.4, Nino 3, and Nino 4, while ENSO has a negative correlation. Due to the fact that the majority of EA regions have a large positive association between IOD and OND rainfall, the effect of IOD on OND rainfall can typically be significant and high compared to other global synoptic systems. This was confirmed by the strongest correlation between IOD and OND rainfall with a high and significant value, as the correlation values of other driving systems are fear. It is documented that IOD has an extreme impact on rainfall during short rainfall (Chang'a et al., 2020; Ratna et al., 2021). There is a high correlation between IOD and OND rainfall in 2019, unlike the year 1997, which indicates a high correlation between both IOD and ENSO and OND rainfall in 1997. The association between EA rainfall and sea-surface temperatures is well documented; several studies have examined this relationship and found that Indian Ocean SSTs significantly influence rainfall variability in East Africa (Doi et al., 2022; Pohlmann & Latif, 2005). The results confirm this association, as the west half of the Indian Ocean exhibits large sea-surface temperature positive anomalies and a significant positive correlation, particularly for the region enclosed by different driving systems. Typically, rising sea surface temperature anomalies across the western Indian Ocean are a signal of a positive IOD condition, which in turn causes rising rainfall activity over the East Africa region. The wind is a key parameter for analyzing extreme weather events, as the convective atmosphere is displaced by the wind (Blau & Ha, 2020). The strong southeasterly winds from South Indian sub-tropical anti-cyclones cause an increase in rainfall in the sub-tropical region of Africa, and EA received high rainfall. This confirms (Mahlobo et al. 2019) that the south-west of the Indian Ocean is a major source of moisture for the subcontinent. This trade wind is associated with the strong low-level Easterly jet over Africa, which was generating easterly waves in regions of low atmospheric pressure that have high intensity (Živić, 2021). For OND 2019, the strong anomalous southeasterly winds from the Indian Ocean strike the majority of the EA as, climatologically, the warm and moist air is moved far away to the EA.

5. Conclusion and Recommendation

This study assessed the driving systems linked to the seasonal rainfall variability throughout the October, November, and December (OND) period in order to identify the actual drivers that cause excessive rainfall over East Africa at the

time of OND 2019. Typically, our process considers seven driving systems in order to determine which driving system has the most effect on the OND rainfall in 2019.

The findings of the influence of driving systems on OND seasonal rainfall vary based on rainfall records, with strong correlations for high rainfall and fair correlations for low rainfall. In general, the entire region of East Africa has a rational positive association with OND rainfall, and these driving systems over the region located around Lake Victoria, south of Uganda, and northwest of Tanzania (region A) and the region located in the center and south of Kenya (region B) exhibit a considerable positive correlation with nearly all driving systems.

The driving systems that have the greatest influence on OND 2019 are IOD, as evidenced by its high correlation coefficient and the SST results. The wind component developed with positive values throughout the OND 2019 period covers the majority of East Africa and delivers warm and wet winds over the region. Relative humidity, geopotential height, vertical velocity, and vorticity all have anomalous values that are indicative of a convective atmosphere, which raises the probability of receiving above-normal rainfall during the OND 2019 period. The outcomes of this paper will help to gather more information on the global synoptic climate systems to better improve predicting the occurrence of extreme rainfall, which enhances weather forecasts as input to the development of adaptation measures to mitigate flood and landslide effects. We urge further studies that can deepen the research on rainfall shortages throughout the OND season.

Data Availability Statement

The study's datasets are open source and can be accessed through the following link: CHIRPS data are available at:

<https://data.chc.ucsb.edu/products/CHIRPS-2.0/>. Various driving system's datasets can be found at <https://psl.noaa.gov/data/timeseries/>. NTA is available at <https://psl.noaa.gov/data/climateindices/list/>. ENSO is accessible at <https://crudata.uea.ac.uk/cru/data//soi/>. The sea surface temperature is available at <https://psl.noaa.gov/data/gridded/data.noaa.ersst.v4.html>.

Author Contributions Statement

Constantine Ingeri: C.I, Wang Wen: W.W, Joseph Ndakize Sebaziga: J.N.S, Vedaste Iyakaremye: V.I, Samuel Ekwacu: S.E, Prosper Ayabagabo: P.A, Anthony Twahirwa A.T and Jonah Kazora: J.K, "Conceptualization part, C.I and W.W; Methodology, C.I. J.N.S, V.I, S.E; software, C.I. J.N.S and V.I; validation, C.I; formal analysis, C.I. J.N.S and V.I; investigation, C.I. J.N.S and V.I; data curation, C.I and P.A; writing original draft preparation, C.I; writing review and editing, C.I. J.N.S, V.I, J.K, A.T visualization, C.I; supervision, W.W; project administration, W.W. All authors have read and agreed to the published version of the manuscript."

Acknowledgements

We thank Mr. Given Bahati Allegre for his valuable support in correction of manuscript.

Conflicts of Interest

The authors declare no conflicts of interest regarding the publication of this paper.

References

- Alexander, M. A., Bladé, I., Newman, M., Lanzante, J. R., Lau, N., & Scott, J.D. (2002). The Atmospheric Bridge: The Influence of ENSO Teleconnections on Air-Sea Interaction over the Global Oceans. *Journal of Climate*, *15*, 2205-2231. [https://doi.org/10.1175/1520-0442\(2002\)015<2205:tabtio>2.0.co;2](https://doi.org/10.1175/1520-0442(2002)015<2205:tabtio>2.0.co;2)
- Balaguru, K., Leung, L. R., Hagos, S. M., & Krishnakumar, S. (2021). An Oceanic Pathway for Madden-Julian Oscillation Influence on Maritime Continent Tropical Cyclones. *NPJ Climate and Atmospheric Science*, *4*, Article No. 52. <https://doi.org/10.1038/s41612-021-00208-4>
- Behera, S. (2021). The Indo-Pacific Climate Dynamics and Teleconnections with a Special Emphasis on the Indian Summer Monsoon Rainfall. *MAUSAM*, *70*, 87-110. <https://doi.org/10.54302/mausam.v70i1.169>
- Black, E. (2005). The Relationship between Indian Ocean Sea-surface Temperature and East African Rainfall. *Philosophical Transactions of the Royal Society A: Mathematical, Physical and Engineering Sciences*, *363*, 43-47. <https://doi.org/10.1098/rsta.2004.1474>
- Black, E., Slingo, J., & Sperber, K. R. (2003). An Observational Study of the Relationship between Excessively Strong Short Rains in Coastal East Africa and Indian Ocean SST. *Monthly Weather Review*, *131*, 74-94. [https://doi.org/10.1175/1520-0493\(2003\)131<0074:aosotr>2.0.co;2](https://doi.org/10.1175/1520-0493(2003)131<0074:aosotr>2.0.co;2)
- Blau, M. T., & Ha, K. J. (2020). The Indian Ocean Dipole and Its Impact on East African Short Rains in Two CMIP5 Historical Scenarios with and without Anthropogenic Influence. *Journal of Geophysical Research: Atmospheres*, *125*, e2020JD033121. <https://doi.org/10.1029/2020jd033121>
- Cai, Y., Chen, Z., & Du, Y. (2022). The Role of Indian Ocean Warming on Extreme Rainfall in Central China during Early Summer 2020: Without Significant El Niño Influence. *Climate Dynamics*, *59*, 951-960. <https://doi.org/10.1007/s00382-022-06165-9>
- Chang'a, L. B., Kijazi, A. L., Mafuru, K. B., Kondowe, A. L., Osima, S. E., Mtongori, H. I. et al. (2020). Assessment of the Evolution and Socio-Economic Impacts of Extreme Rainfall Events in October 2019 over the East Africa. *Atmospheric and Climate Sciences*, *10*, 319-338. <https://doi.org/10.4236/acs.2020.103018>
- Dezfuli, A. K., & Nicholson, S. E. (2013). The Relationship of Rainfall Variability in Western Equatorial Africa to the Tropical Oceans and Atmospheric Circulation. Part II: The Boreal Autumn. *Journal of Climate*, *26*, 66-84. <https://doi.org/10.1175/jcli-d-11-00686.1>
- Dieppois, B., Rouault, M., & New, M. (2015). The Impact of ENSO on Southern African Rainfall in CMIP5 Ocean Atmosphere Coupled Climate Models. *Climate Dynamics*, *45*, 2425-2442. <https://doi.org/10.1007/s00382-015-2480-x>
- Doi, T., Behera, S. K., & Yamagata, T. (2022). On the Predictability of the Extreme Drought in East Africa during the Short Rains Season. *Geophysical Research Letters*,

- 49, e2022GL100905. <https://doi.org/10.1029/2022gl100905>
- Eichhorn, A., & Bader, J. (2016). Impact of Tropical Atlantic Sea-Surface Temperature Biases on the Simulated Atmospheric Circulation and Precipitation over the Atlantic Region: An ECHAM6 Model Study. *Climate Dynamics*, 49, 2061-2075. <https://doi.org/10.1007/s00382-016-3415-x>
- Endris, H. S., Lennard, C., Hewitson, B., Dosio, A., Nikulin, G., & Artan, G. A. (2018). Future Changes in Rainfall Associated with ENSO, IOD and Changes in the Mean State over Eastern Africa. *Climate Dynamics*, 52, 2029-2053. <https://doi.org/10.1007/s00382-018-4239-7>
- Finney, D. L., Marsham, J. H., Walker, D. P., Birch, C. E., Woodhams, B. J., Jackson, L. S. et al. (2019). The Effect of Westerlies on East African Rainfall and the Associated Role of Tropical Cyclones and the Madden-Julian Oscillation. *Quarterly Journal of the Royal Meteorological Society*, 146, 647-664. <https://doi.org/10.1002/qj.3698>
- Green, B., Marshall, J., & Donohoe, A. (2017). Twentieth Century Correlations between Extratropical SST Variability and ITCZ Shifts. *Geophysical Research Letters*, 44, 9039-9047. <https://doi.org/10.1002/2017gl075044>
- Indeje, M., Semazzi, F. H. M., & Ogallo, L. J. (2000). ENSO Signals in East African Rainfall Seasons. *International Journal of Climatology*, 20, 19-46. [https://doi.org/10.1002/\(sici\)1097-0088\(200001\)20:1<19::aid-joc449>3.0.co;2-0](https://doi.org/10.1002/(sici)1097-0088(200001)20:1<19::aid-joc449>3.0.co;2-0)
- Jury, M. R., Matari, E., & Matitu, M. (2008). Equatorial African Climate Teleconnections. *Theoretical and Applied Climatology*, 95, 407-416. <https://doi.org/10.1007/s00704-008-0018-4>
- Kai, K. H., Kijazi, A. L., & Osima, S. E. (2020). An Assessment of the Seasonal Rainfall and Its Societal Implications in Zanzibar Islands during the Season of October to December, 2019. *Atmospheric and Climate Sciences*, 10, 509-529. <https://doi.org/10.4236/acs.2020.104026>
- Kavishe, G. M., & Limbu, P. T. S. (2020). Variation of October to December Rainfall in Tanzania and Its Association with Sea Surface Temperature. *Arabian Journal of Geosciences*, 13, Article No. 534. <https://doi.org/10.1007/s12517-020-05535-z>
- Kebacho, L. L. (2021). Anomalous Circulation Patterns Associated with 2011 Heavy Rainfall over Northern Tanzania. *Natural Hazards*, 109, 2295-2312. <https://doi.org/10.1007/s11069-021-04920-5>
- Kebacho, L. L. (2022). The Role of Tropical Cyclones Idai and Kenneth in Modulating Rainfall Performance of 2019 Long Rains over East Africa. *Pure and Applied Geophysics*, 179, 1387-1401. <https://doi.org/10.1007/s00024-022-02993-2>
- Kidson, J. W. (1977). African Rainfall and Its Relation to the Upper Air Circulation. *Quarterly Journal of the Royal Meteorological Society*, 103, 441-456. <https://doi.org/10.1256/smsqj.43704>
- King'uzi, P., & Tilwebwa, S. (2019). Inter-annual Variability of March to May Rainfall over Tanzania and Its Association with Atmospheric Circulation Anomalies. *Geographica Pannonica*, 23, 147-161. <https://doi.org/10.5937/gp23-22430>
- Klein, F., & Goosse, H. (2017). Reconstructing East African Rainfall and Indian Ocean Sea Surface Temperatures over the Last Centuries Using Data Assimilation. *Climate Dynamics*, 50, 3909-3929. <https://doi.org/10.1007/s00382-017-3853-0>
- Kolstad, E. W., & MacLeod, D. (2022). Lagged Oceanic Effects on the East African Short Rains. *Climate Dynamics*, 59, 1043-1056. <https://doi.org/10.1007/s00382-022-06176-6>
- Krüzselyi, I., Bartholy, J., Horányi, A., Pieczka, I., Pongrácz, R., Szabó, P. et al. (2011). The Future Climate Characteristics of the Carpathian Basin Based on a Regional Cli-

- mate Model Mini-Ensemble. *Advances in Science and Research*, 6, 69-73. <https://doi.org/10.5194/asr-6-69-2011>
- Latif, M., & Grötzner, A. (2000). The Equatorial Atlantic Oscillation and Its Response to Enso. *Climate Dynamics*, 16, 213-218. <https://doi.org/10.1007/s003820050014>
- Latif, M., Dommenges, D., Dima, M., & Grötzner, A. (1999). The Role of Indian Ocean Sea Surface Temperature in Forcing East African Rainfall Anomalies during December-January 1997/98. *Journal of Climate*, 12, 3497-3504. [https://doi.org/10.1175/1520-0442\(1999\)012<3497:troios>2.0.co;2](https://doi.org/10.1175/1520-0442(1999)012<3497:troios>2.0.co;2)
- Liu, Y., Chiang, J. C. H., Chou, C., & Patricola, C. M. (2014). Atmospheric Teleconnection Mechanisms of Extratropical North Atlantic SST Influence on Sahel Rainfall. *Climate Dynamics*, 43, 2797-2811. <https://doi.org/10.1007/s00382-014-2094-8>
- Lüdecke, H., Müller-Plath, G., Wallace, M. G., & Lüning, S. (2021). Decadal and Multi-decadal Natural Variability of African Rainfall. *Journal of Hydrology: Regional Studies*, 34, Article ID: 100795. <https://doi.org/10.1016/j.ejrh.2021.100795>
- Lyon, B. (2020). Biases in CMIP5 Sea Surface Temperature and the Annual Cycle of East African Rainfall. *Journal of Climate*, 33, 8209-8223. <https://doi.org/10.1175/jcli-d-20-0092.1>
- Mahlobo, D. D., Ndarana, T., Grab, S., & Engelbrecht, F. (2018). Integrated Climatology and Trends in the Subtropical Hadley Cell, Sunshine Duration and Cloud Cover over South Africa. *International Journal of Climatology*, 39, 1805-1821. <https://doi.org/10.1002/joc.5917>
- Mbigi, D., & Xiao, Z. (2023). Southern Annular Mode: A New Factor Impacts the East African Short Rains after the Early 1990s. *Journal of Climate*, 36, 5511-5525. <https://doi.org/10.1175/jcli-d-22-0613.1>
- McHugh, M. J., & Rogers, J. C. (2001). North Atlantic Oscillation Influence on Precipitation Variability around the Southeast African Convergence Zone. *Journal of Climate*, 14, 3631-3642. [https://doi.org/10.1175/1520-0442\(2001\)014<3631:naoiop>2.0.co;2](https://doi.org/10.1175/1520-0442(2001)014<3631:naoiop>2.0.co;2)
- Moron, V. (1997). Trend, Decadal and Interannual Variability in Annual Rainfall of Subequatorial and Tropical North Africa (1900-1994). *International Journal of Climatology*, 17, 785-805. [https://doi.org/10.1002/\(sici\)1097-0088\(19970630\)17:8<785::aid-joc153>3.0.co;2-i](https://doi.org/10.1002/(sici)1097-0088(19970630)17:8<785::aid-joc153>3.0.co;2-i)
- Müller, W. A., & Roeckner, E. (2008). ENSO Teleconnections in Projections of Future Climate in ECHAM5/MPI-OM. *Climate Dynamics*, 31, 533-549. <https://doi.org/10.1007/s00382-007-0357-3>
- Mutai, C. C., Ward, M. N., & Colman, A. W. (1998). Towards the Prediction of the East Africa Short Rains Based on Sea-Surface Temperature-Atmosphere Coupling. *International Journal of Climatology*, 18, 975-997. [https://doi.org/10.1002/\(sici\)1097-0088\(199807\)18:9<975::aid-joc259>3.3.co;2-1](https://doi.org/10.1002/(sici)1097-0088(199807)18:9<975::aid-joc259>3.3.co;2-1)
- Muthoni, F. K., Odongo, V. O., Ochieng, J., Mugalavai, E. M., Mourice, S. K., Hoesche-Zeledon, I. et al. (2018). Long-Term Spatial-Temporal Trends and Variability of Rainfall over Eastern and Southern Africa. *Theoretical and Applied Climatology*, 137, 1869-1882. <https://doi.org/10.1007/s00704-018-2712-1>
- Ngoma, H., Wen, W., Ojara, M., & Ayugi, B. (2021). Assessing Current and Future Spatiotemporal Precipitation Variability and Trends over Uganda, East Africa, Based on CHIRPS and Regional Climate Model Datasets. *Meteorology and Atmospheric Physics*, 133, 823-843. <https://doi.org/10.1007/s00703-021-00784-3>
- Nicholson, S. E. (2017). Climate and Climatic Variability of Rainfall over Eastern Africa. *Reviews of Geophysics*, 55, 590-635. <https://doi.org/10.1002/2016rg000544>
- Nicholson, S. E. (2019). A Review of Climate Dynamics and Climate Variability in East-

- ern Africa. In T. C Johnson, & E. O Odada (Eds.), *Limnology, Climatology and Paleoclimatology of the East African Lakes*. Routledge.
<https://doi.org/10.1201/9780203748978-2>
- Nicholson, S. E., & Dezfuli, A. K. (2013). The Relationship of Rainfall Variability in Western Equatorial Africa to the Tropical Oceans and Atmospheric Circulation. Part I: The Boreal Spring. *Journal of Climate*, *26*, 45-65.
<https://doi.org/10.1175/jcli-d-11-00653.1>
- Nicholson, S. E., & Selato, J. C. (2000). The Influence of La Nina on African Rainfall. *International Journal of Climatology*, *20*, 1761-1776.
[https://doi.org/10.1002/1097-0088\(20001130\)20:14<1761::aid-joc580>3.0.co;2-w](https://doi.org/10.1002/1097-0088(20001130)20:14<1761::aid-joc580>3.0.co;2-w)
- Nicholson, S. E., Fink, A. H., Funk, C., Klotter, D. A., & Satheesh, A. R. (2022). Meteorological Causes of the Catastrophic Rains of October/November 2019 in Equatorial Africa. *Global and Planetary Change*, *208*, Article ID: 103687.
<https://doi.org/10.1016/j.gloplacha.2021.103687>
- Nyenzi, B. S. (1988). Mechanisms of East African Rainfall Variability. *Atmospheric Science*, *49*, 2232.
- Ogallo, L. J. (1988). Relationships between Seasonal Rainfall in East Africa and the Southern Oscillation. *Journal of Climatology*, *8*, 31-43.
<https://doi.org/10.1002/joc.3370080104>
- Ogallo, L. J. (1989). The Spatial and Temporal Patterns of the East African Seasonal Rainfall Derived from Principal Component Analysis. *International Journal of Climatology*, *9*, 145-167. <https://doi.org/10.1002/joc.3370090204>
- Ongoma, V., Chen, H., & Gao, C. (2017). Projected Changes in Mean Rainfall and Temperature over East Africa Based on CMIP5 Models. *International Journal of Climatology*, *38*, 1375-1392. <https://doi.org/10.1002/joc.5252>
- Onyutha, C. (2016). Geospatial Trends and Decadal Anomalies in Extreme Rainfall over Uganda, East Africa. *Advances in Meteorology*, *2016*, Article ID: 6935912.
<https://doi.org/10.1155/2016/6935912>
- Otieno, G., Mutemi, J., Opijah, F., Ogallo, L., & Omondi, H. (2018). The Impact of Cumulus Parameterization on Rainfall Simulations over East Africa. *Atmospheric and Climate Sciences*, *8*, 355-371. <https://doi.org/10.4236/acs.2018.83024>
- Palmer, P. I., Wainwright, C. M., Dong, B., Maidment, R. I., Wheeler, K. G., Gedney, N., et al. (2023). Drivers and Impacts of Eastern African Rainfall Variability. *Nature Reviews Earth & Environment*, *4*, 254-270. <https://doi.org/10.1038/s43017-023-00397-x>
- Philippon, N., Baron, C., Boyard-Micheau, J., Adde, A., Leclerc, C., Mwangera, C. et al. (2015). Climatic Gradients along the Windward Slopes of Mount Kenya and Their Implication for Crop Risks. Part 2: Crop Sensitivity. *International Journal of Climatology*, *36*, 917-932. <https://doi.org/10.1002/joc.4394>
- Pohlmann, H., & Latif, M. (2005). Atlantic versus Indo-pacific Influence on Atlantic-European Climate. *Geophysical Research Letters*, *32*, L05707.
<https://doi.org/10.1029/2004gl021316>
- Preethi, B., Sabin, T. P., Adedoyin, J. A., & Ashok, K. (2015). Impacts of the ENSO Modoki and Other Tropical Indo-Pacific Climate-Drivers on African Rainfall. *Scientific Reports*, *5*, Article No. 16653. <https://doi.org/10.1038/srep16653>
- Ratna, S. B., Cherchi, A., Osborn, T. J., Joshi, M., & Uppara, U. (2021). The Extreme Positive Indian Ocean Dipole of 2019 and Associated Indian Summer Monsoon Rainfall Response. *Geophysical Research Letters*, *48*, e2020GL091497.
<https://doi.org/10.1029/2020gl091497>

- Ren, H., Zuo, J., & Deng, Y. (2018). Statistical Predictability of Niño Indices for Two Types of Enso. *Climate Dynamics*, *52*, 5361-5382. <https://doi.org/10.1007/s00382-018-4453-3>
- Ropelewski, C. F., & Halpert, M. S. (1987). Global and Regional Scale Precipitation Patterns Associated with the El Niño/southern Oscillation. *Monthly Weather Review*, *115*, 1606-1626. [https://doi.org/10.1175/1520-0493\(1987\)115<1606:garspp>2.0.co;2](https://doi.org/10.1175/1520-0493(1987)115<1606:garspp>2.0.co;2)
- Roy, I., Mliwa, M., & Troccoli, A. (2023). Important Drivers of East African Monsoon Variability and Improving Rainy Season Onset Prediction. *Natural Hazards*, *120*, 429-445. <https://doi.org/10.1007/s11069-023-06223-3>
- Shilenje, Z. W., & Ogwang, B. A. (2015). The Role of Kenya Meteorological Service in Weather Early Warning in Kenya. *International Journal of Atmospheric Sciences*, *2015*, Article ID: 302076. <https://doi.org/10.1155/2015/302076>
- Shrivastava, A. C., & Umar, M. (2023). The Impact of Big Data on Climate Change. In *2023 International Conference on Innovative Data Communication Technologies and Application (ICIDCA)* (pp. 481-488). IEEE. <https://doi.org/10.1109/icidca56705.2023.10099659>
- Varada, V. (2005). *East African Hydroclimatic Variability: 1950-1999*. Master's Theses, Louisiana State University.
- Vashisht, A., & Zaitchik, B. (2022). Modulation of East African Boreal Fall Rainfall: Combined Effects of the Madden-Julian Oscillation (MJO) and El Niño-Southern Oscillation (ENSO). *Journal of Climate*, *35*, 2019-2034. <https://doi.org/10.1175/jcli-d-21-0583.1>
- Wainwright, C. M., Finney, D. L., Kilavi, M., Black, E., & Marsham, J. H. (2020). Extreme Rainfall in East Africa, October 2019-January 2020 and Context under Future Climate Change. *Weather*, *76*, 26-31. <https://doi.org/10.1002/wea.3824>
- Wenegrat, J. O., Bonanno, E., Rack, U., & Gebbie, G. (2022). A Century of Observed Temperature Change in the Indian Ocean. *Geophysical Research Letters*, *49*, e2022GL098217. <https://doi.org/10.1029/2022gl098217>
- Woodward, G., Bonada, N., Brown, L. E., Death, R. G., Durance, I., Gray, C. et al. (2016). The Effects of Climatic Fluctuations and Extreme Events on Running Water Ecosystems. *Philosophical Transactions of the Royal Society B: Biological Sciences*, *371*, Article ID: 20150274. <https://doi.org/10.1098/rstb.2015.0274>
- Yang, J., Lv, Z., Richter, I., Zhang, Y., & Lin, X. (2022) Inter-Model Spread of North Tropical Atlantic Trans-Basin Effect Substantially Biases Tropical Pacific Sea Surface Temperature Multiyear Prediction. *Geophysical Research Letters*, *49*, e2022GL098620. <https://doi.org/10.1029/2022gl098620>
- Zhang, R., & Delworth, T. L. (2006). Impact of Atlantic Multidecadal Oscillations on India/Sahel Rainfall and Atlantic Hurricanes. *Geophysical Research Letters*, *33*, L17712. <https://doi.org/10.1029/2006gl026267>
- Živić, T. (2021). Encyclopædia Britannica Online. *Studia lexicographica*, *14*, 109-123. <https://doi.org/10.33604/sl.14.27.6>
- Dezfuli, A. K., & Nicholson, S. E. (2011). A Note on Long-Term Variations of the African Easterly Jet. *International Journal of Climatology*, *31*, 2049-2054. <https://doi.org/10.1002/joc.2209>
- Gunta, S., & Bhat, H. (2022). The Response of Geopotential Height Anomalies to El Niño and La Niña Conditions and Their Implications to Seasonal Rainfall Variability over the Horn of Africa. *Atmospheric and Climate Sciences*, *12*, 475-492. <https://doi.org/10.4236/acs.2022.122028>

Ogwang, B. A., Chen, H., Tan, G., Ongoma, V., & Ntwali, D. (2015). Diagnosis of East African Climate and the Circulation Mechanisms Associated with Extreme Wet and Dry Events: A Study Based on RegCM4. *Arabian Journal of Geosciences*, 8, 10255-10265. <https://doi.org/10.1007/s12517-015-1949-6>